International Journal of Architectural, Civil and Construction Sciences
ISSN: 2415-1734
Vol:13, No:1, 2019

Development of Equivalent Inelastic Springs to Model C-Devices

Oday Al-Mamoori, J. Enrique Martinez-Rueda

***Abstract*—**'C' shape yielding devices (C-devices) are effective tools for introducing supplemental sources of energy dissipation by hysteresis. Studies have shown that C-devices made of mild steel can be successfully applied as integral parts of seismic retrofitting schemes. However, explicit modelling of these devices can become cumbersome, expensive and time consuming. The device under study in this article has been previously used in non-invasive dissipative bracing for seismic retrofitting. The device is cut from a mild steel plate and has an overall shape that resembles that of a rectangular portal frame with circular interior corner transitions to avoid stress concentration and to control the extension of the dissipative region of the device. A number of inelastic finite element (FE) analyses using either inelastic 2D plane stress elements or inelastic fibre frame elements are reported and used to calibrate a 1D equivalent inelastic spring model that effectively reproduces the cyclic response of the device. The more elaborate FE model accounts for the frictional forces developed between the steel plate and the bolts used to connect the C-device to structural members. FE results also allow the visualization of the inelastic regions of the device where energy dissipation is expected to occur. FE analysis results are in a good agreement with experimental observations.

***Keywords*—**C-device, equivalent nonlinear spring, FE analyses, reversed cyclic tests.

I. Introduction

MANY types of C-device have been developed over past decades such as the C-device with rectangular cross section [1], circular cross section [2], and curved C-devices [3]-[5]. C-devices made from steel plates are another instance of yield hysteretic energy dissipation devices (HEDD) incorporated in the Cromwell Bridge, New Zealand [4]. Generally, C-devices are fabricated from either a solid steel profile or cut from a mild steel plate. Among these devices, the C-device described in [6], and shown in Fig. 1, was proposed as an alternative cheaper C-device. This is due to its simpler geometry. This device is fabricated from a mild steel plate using a simple cutting procedure [6]. It has an overall rectangular shape with circular interior corner transitions of radius r and a dissipative region of length L_d. The circular transitions are located at both sides of the C-device to reduce stress concentration at the interior corners so that inelastic deformation occurs mainly in the dissipative region of device.

The distance between the longitudinal axis of the device (x_d-x_d) and longitudinal axis of yielding region (x-x) results in the eccentricity L_y. Although the above C-device appears well conceived, further analytical and experimental studies of the device alone are clearly missing. Reference [6] describes a cyclic test of this device only as an integral part of a dissipative bracing of low structural "invasion". Although this test clearly revealed the dissipation capacity of the device and the visual demarcation of the yielding region (dissipative region), no detailed instrumentation was used to monitor specifically the device response and no tests were conducted on the device alone.

This paper introduces a methodology to calibrate the properties of an equivalent nonlinear inelastic spring that reproduces the expected hysteretic response of a C-device. Furthermore, an elaborate model of the C-device using two-dimensional (2D) inelastic finite element (FE) analysis of solid elements under plane stress is presented. Results obtained from FE analyses are compared against those obtained from experimental test results under monotonic and cyclic loads.

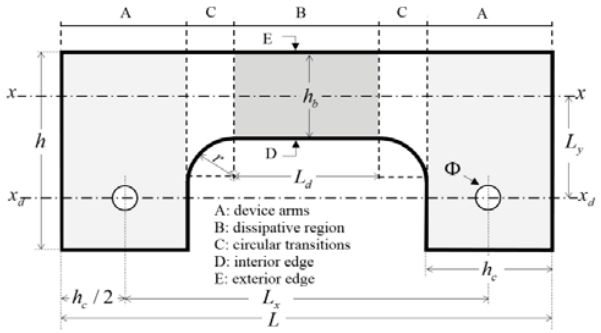

Fig. 1 C-device proposed by [6]

II. Modelling of the C-Device (Individual)

A. Geometry of the Devices

To assess the effect of L_d and the aspect ratio of the dissipative region on the performance of the C-device, a number of FE models of the device were initially studied using SAP2000 [7]. Table I summarizes the geometric dimensions of the FE models of C-devices with thickness *t* equal to 10 mm.

TABLE I
Geometric Dimensions of Models

No	Device name	L_d [mm]	r [mm]	h_b [mm]	h_c [mm]	L_y [mm]	L [mm]	L_x [mm]	h [mm]	Ø [mm]
1	$R90$-0.80h_b	140	90	175	240	206	800	560	400	50
2	$R90$-1.37h_b	240	90	175	240	206	900	660	400	50
3	$R90$-1.60h_b	280	90	175	240	206	940	700	400	50

Oday Al-Mamoori graduated from the University of Babylon, Iraq and is currently a PhD student at the University of Brighton, Brighton, Moulsecoomb place, BN24HQ, UK (e-mail: ohh10@ brighton.ac.uk).

Dr. Juan Enrique Martinez-Rueda is a Senior Lecturer in Earthquake Engineering and Structural Dynamics at the University of Brighton, Lewes Road Cockcroft Bldg, BN24GJ, UK (e-mail: jem11@bton.ac.uk).

B. FE Model of the C-Device

The device under study was modelled using an assembly of the three regions identified in Fig. 1 as:

1) Region A is denoted as elastic region.
2) Region C is subdivided into 20 nonlinear fibre elements with rectangular cross sections of variable depths.
3) Region B is subdivided into five nonlinear fibre elements with constant cross section. A number of convergence studies showed there was no need to refine FE mesh further.

For the inelastic regions, 30 fibres were used to model the cross section. Fig. 2 shows the simplified model of the C-device. In general, the C-device is modelled using an assembly of 45 inelastic fibre elements. A roller joint is situated on the right end of the device model while a pinned joint is placed on the left end. Basically, the roller joint allows the device to deform under imposed displacements (Δ) along the longitudinal axis of the device (see Fig. 1) while the pinned joint allows free rotations. Rigid links are used to model the device arms (region A in Fig. 1).

Steel was modelled using its cyclic curve as the backbone of hysteretic loops assuming kinematic hardening. The yield strength of steel was taken as 275 MPa. The parameters of the cyclic curve of steel (K' and n') were obtained based on parameters of the monotonic stress-strain curve (e.g. steel model shown in [8]). However, the cyclic yield strength requires calibration [9]. The cyclic curve was estimated based on the equation suggested in [10] given below:

$$\sigma_s = K' \left(\varepsilon_p\right)^{n'} \quad (1)$$

where σ_s and ε_p are the normal stress and plastic strain of steel, respectively.

In the analyses reported here, the cyclic yield strength f_y' and the cyclic yield strain ε_y' for mild steel were taken as 206 MPa and 0.001031, respectively. The parameters n' and K' of the cyclic curve were calibrated to be 0.12 and 476 MPa, respectively.

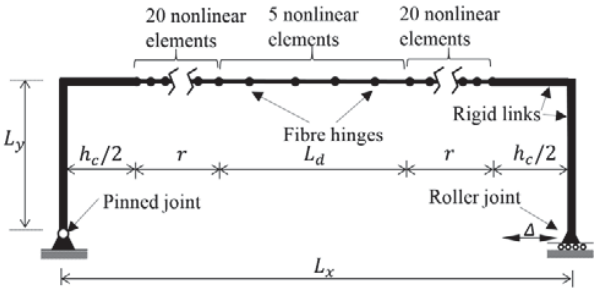

Fig. 2 FE mesh of C-device model

C. Study of the Response of Individual C-Devices

Fig. 3 shows the influence of the extension of the dissipative region L_d on the tensile monotonic response of the C-device with P-Delta effects neglected. In general, the shorter the length of the dissipative region, the higher the strength of the device. However, the difference in strength is not significant (a 2% average maximum difference was identified).

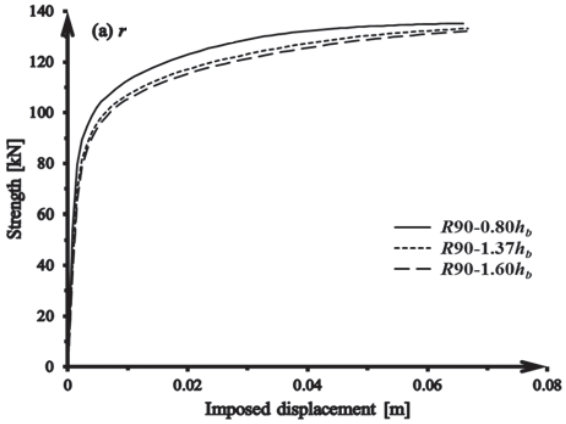

Fig. 3 Influence of L_d on the monotonic behaviour of the C-device under monotonic loading

D. Modelling of the C-Device Using Equivalent Nonlinear Inelastic Springs

To model the nonlinear behaviour of the C-device in a simpler way, a nonlinear inelastic spring with kinematic hardening can be used. This approach makes the analyses more efficient in terms of computational effort. The kinematic hardening model can reproduce multi-nonlinear plasticity with several types of hysteretic response. The equivalent nonlinear spring (see Fig. 4) is bounded by two joints and has a nonlinear axial stiffness. The pushover response of a more detailed model of the device (e.g. Fig. 3) can be used to define the properties of the equivalent spring.

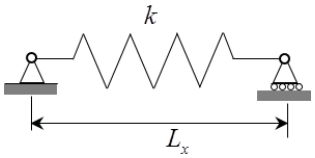

Fig. 4 Sketch of an equivalent nonlinear spring

E. Response under Reversed Cyclic Loading

A comparison of the cyclic response of the C-device for two different device models has been established. The cyclic analysis was conducted by imposing the displacement controlled load history shown in Fig. 5 (a).

As shown in Fig. 5 (b), the observed hysteretic behaviour of the simplified model of the C-device $R90\text{-}1.6h_b$ (see Table I) is similar to that of the equivalent nonlinear spring model. Fig. 5 (b) also confirms that the strength developed by the device depends on the imposed ductility. Thus, it can be seen that when a displacement ductility of $14\Delta_y$ was imposed, the strength of the C-device was approximately 30% in excess of that at the yield condition obtained from the monotonic response.

A more precise understanding of the behaviour of the C-device for two different device models can be established in

terms of energy dissipation and stiffness degradation comparisons. Fig. 6 illustrates the evolution of the hysteretic energy dissipated by both models. The total hysteretic energy dissipated by the device at the end of the load history was around 40 kN-m. Fig. 7 illustrates the secant stiffness assessed peak-to-peak of a given hysteresis loop. At the end of the history, the secant stiffness is just 11% of the value obtained for the first cycle. Both Figs. 6 and 7 confirm that the equivalent nonlinear spring effectively reproduces the behaviour of a more elaborate and detailed model of the device.

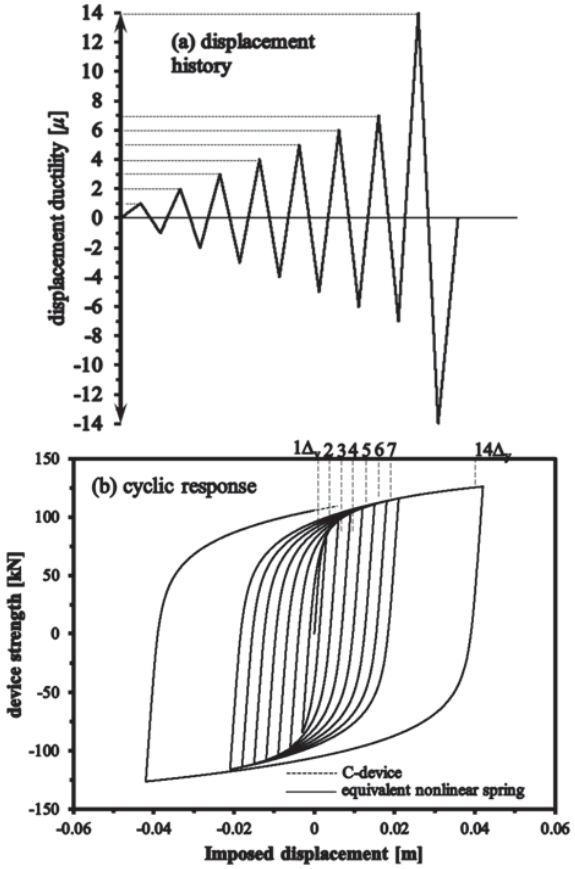

Fig. 5 Displacement history and comparison of cyclic response of the C-device for two different device models

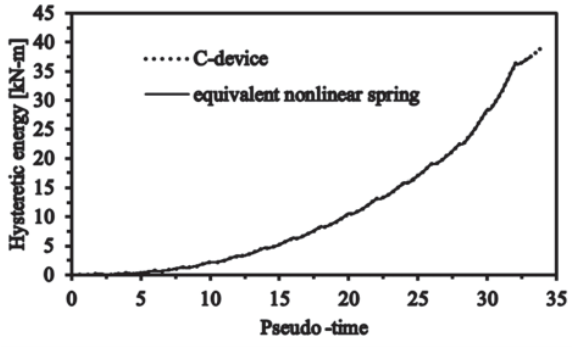

Fig. 6 Comparison of the hysteretic energy dissipated by C-device for two different device models under reversed cyclic loading

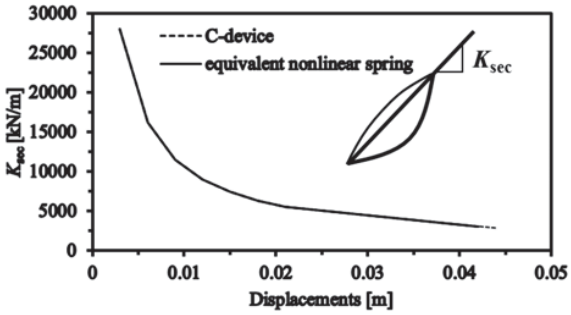

Fig. 7 Comparison of predicted stiffness degradation using different device models under reversed cyclic loading

III. Modelling of the C-Device Connected to RC Members

A. Definition of Member Models

Fig. 8 shows RC column models with two different approaches to model the devices. The column models represent a cantilever column supporting a lumped mass M at the top. The mass was selected so that the initial period of the model is 0.4 sec. As the columns have a pinned joint at their base the attached devices provide strength and stability to the system.

A set of rigid links with length equal to half of the column cross section depth (see Fig. 9) is used to connect the devices to the column while two more rigid links are provided to connect the devices to the foundation. Fig. 9 defines the required lengths e_x and e_y of the rigid links. The assembly of connection plates shown in Fig. 9 must have adequate strength and stiffness to achieve the maximum efficiency of the C-devices. The assembly of connection plates consisting of anchor bolts and base plates with pinned joints must be designed to resist forces higher than the yield strength of devices; this with the aim of concentrating energy dissipation only in the HEDDs [11]. The RC columns were modelled using a fibre element approach to define the response of the plastic hinge regions. More detailed information about this model can be found in [9].

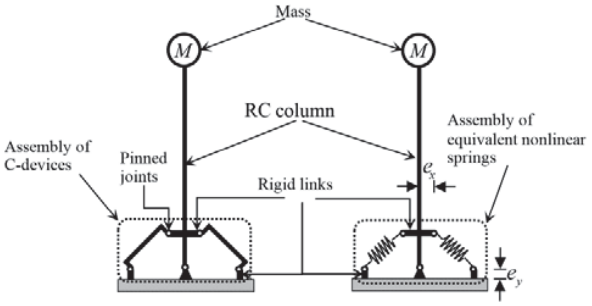

Fig. 8 Incorporation of C-devices around a pinned column base

B. Response under Monotonic Lateral Loading

The pushover responses of the column models are illustrated in Fig. 10. These responses were obtained by applying a lateral displacement of 0.25 m at the top of the columns. The yield displacement and maximum strength of the column model using C-devices $R90\text{-}1.6h_b$ (refer to Table I) with a thickness of 10 mm were found to be 0.011 m and 123.0 kN, respectively.

A clear similarity in the two pushover responses can be observed.

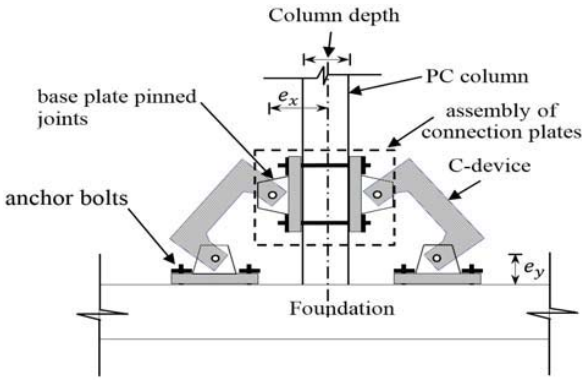

Fig. 9 Eccentricities e_x and e_y

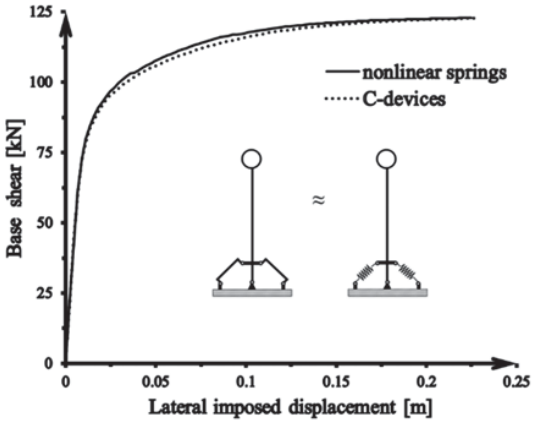

Fig. 10 Comparison of pushover response of the cantilever column with C-devices for two different device models

C. Response under Earthquake Ground Motion (EGM)

A nonlinear time history analysis of the column model using two simplified models subjected to the El Centro 1940, NS earthquake record was performed assuming zero viscous damping. The analysis considered only the first 12 seconds of the EGM including 5 seconds of zero acceleration, as shown in Fig. 11. This allowed the estimation of residual displacements. Three intensity levels were considered: 100% intensity (PGA = 0.32g), 200% intensity (PGA = 0.64g), and 300% intensity (PGA = 0.96g). The first intensity is representative of a ground motion that may initiate yielding in the devices. The second and third intensities are representative of ground motions that produce significant yielding in the devices.

It is observed in Fig. 12 that both models have virtually the same displacement response. The maximum displacement for both models was found to be -0.037 m, -0.093 m and -0.18 m for EGM scaled to PGA = 0.32 g, 0.64 g and 0.96 g, respectively. It is observed that the greater the intensity of the EGM, the larger the resulting residual displacements are. Also, the hysteretic response shows very close agreement between the two models as shown in Fig. 13. A more exhaustive set of results can be found elsewhere [9]

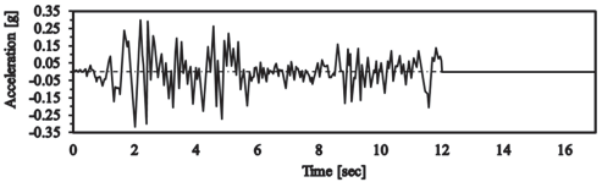

Fig. 11 El Centro NS 1940 EGM

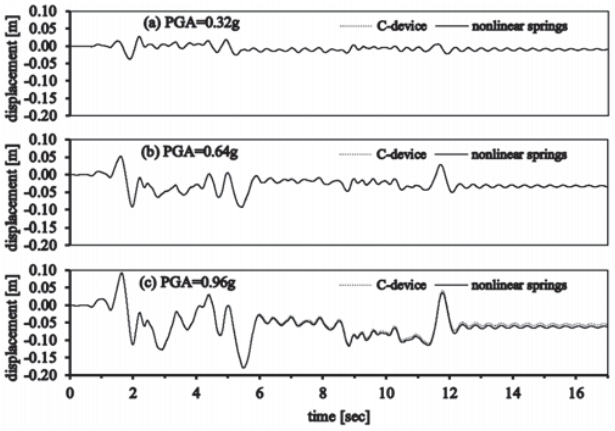

Fig. 12 Comparison of displacement response time-history of the cantilever column with C-devices for two different device models under El Centro EGM scaled at three intensity levels

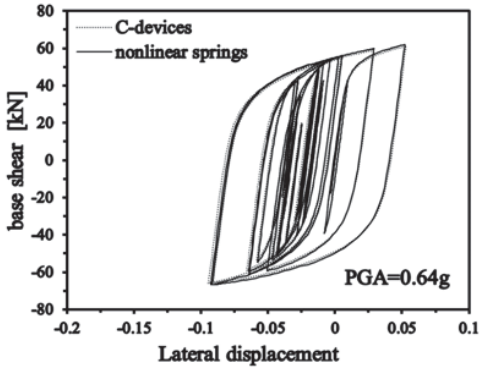

Fig. 13 Comparison of hysteretic behaviour of the cantilever column with C-devices for two different device models under El Centro EGM subjected to PGA = 0.64g

IV. Test Results vs. FE Simulations of the C-Device

This section presents comparative examples between the experimental results and the numerical results obtained from FE analyses conducted in SAP2000 [7] and ADINA [12], respectively. In the interest of brevity only one example is given for both SAP2000 and ADINA. A more exhaustive set of results can be found elsewhere [9].

Dimensions of the C-device used for testing and modelling are summarized in Table II. A mild steel plate with the grade S275 and a plate thickness of 10 mm was used to produce the C-device. The cyclic curve of steel as described in Section II

was used to model the steel hysteretic response of the C-device.

TABLE II
GEOMETRIC DIMENSIONS USED FOR TESTING AND MODELLING OF THE C-DEVICE

No	Device Name	L_d [mm]	r [mm]	h_b [mm]	h_c [mm]	L_y [mm]	L [mm]	L_x [mm]	h [mm]	$\emptyset$ [mm]
1	$R50\text{-}1h_b$	58	50	58	80	65	318	238	130	20

A. Test Results vs. SAP2000 Model

Fig. 14 shows a comparative example of test results vs. numerical predictions obtained with SAP2000 using an assembly of inelastic fibre elements (see model shown in Fig. 2). It is observed that numerical model was capable of predicting closely enough the cyclic response of the C-device.

The loading and unloading stiffness predicted by the numerical model are slightly higher than those observed in the test. However, the maximum strength of the specimen at the early and post-yield hysteretic responses obtained from the numerical model are both in accordance with the observed experimental behaviour.

Based on the comparative example shown in Fig. 14, the FE model built in SAP2000 can be considered reliable to predict the cyclic behaviour of the C-devices.

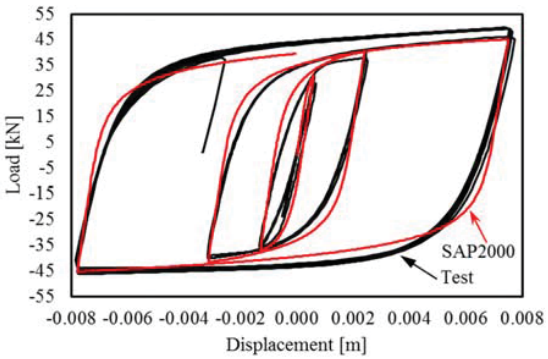

Fig. 14 Comparison example: test *vs.* numerical prediction

B. Test Results vs. ADINA Model

Inelastic 2D plane stress solid elements were used to model the C-device in ADINA. A similar modelling approach has been widely used by other researchers [13]-[16]. The 2D solid elements under plane stress were defined in the ZY plane with a constant thickness element (10 mm). This elaborate FE model was meshed by using 8-node quadrilateral finite elements based on the criteria described in [13]. To identify whether the mesh used is fine enough, the criterion of the stress band method [13] was applied. The FE model also accounts for the frictional forces developed between the steel plate conforming the C-device and the bolts connecting the device to the base plates. The approach to model the frictional interaction between the bolt and the device was based on assuming that C-device elements are selected to be the 'contactor' (deformable surface) and the bolt is defined as a rigid surface. Additionally, within the contact pair, the nodes of the device elements are prevented from penetrating the segments of the bolt surface but not vice versa. A zero gap is also assumed at the contact surface, which means that the device elements are idealised as touching the bolt surface. A friction coefficient equal to 0.4 [15] was assigned to the contact elements when the friction is considered.

Fig. 15 shows a comparison of pushover response for models implemented in SAP2000 and ADINA. A very good agreement is observed in terms of strength and stiffness for the entire range of displacements.

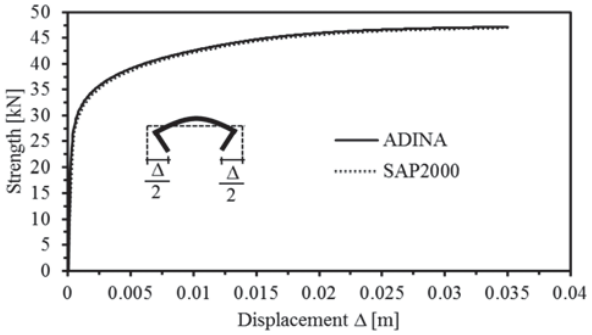

Fig. 15 Comparison of a FE analysis predictions

The comparison between a FE model built in ADINA and the experimental test, illustrated in Fig. 16 demonstrated that simulations can successfully predict the behaviour of the tested C-devices. Both deformed shapes are quite similar and resulted in a good agreement. As can be seen from the figures, inelastic stress is mainly covering the dissipative region of the device and the stress intensity in the circular transition regions is relatively low. This model is able to capture the expected stress distribution. Similar agreements were also observed with the other device tests [9].

Fig. 16 also confirms that the original intended effect of the circular transitions [6] actually occur as yielding takes place primarily inside the dissipative region. In fact, the distribution of the von Mises stress presents the most intense inelastic values mainly over a large volume of the dissipative region. Mild yielding is evident over a small region of the circular transition.

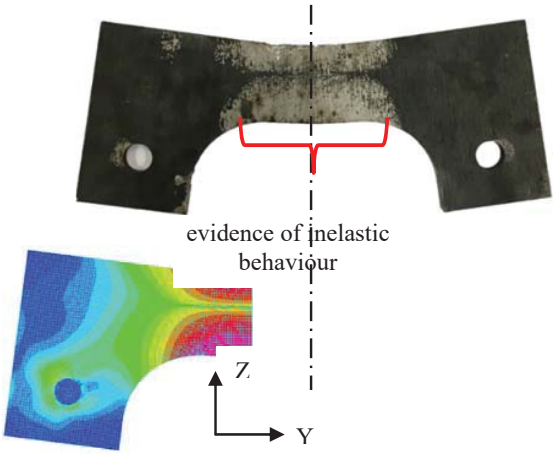

Fig. 16 Comparison of stress distribution between test observations and von Mises stress predicted with ADINA

V. Conclusion

This work has shown that the use of equivalent nonlinear springs is an effective approach to model the monotonic and cyclic behaviour of C-devices. The properties of these springs can be calibrated based on the results obtained from inelastic FE analysis or tests of the C-device. In fact, test results of the device reported here showed good agreement with numerical predictions obtained with two FE models of different level of sophistication. It was also observed that the simpler FE model built in SAP2000 (relying primarily on a non-linear fibre element formulation) showed good agreement with the elaborate model built in ADINA (which made used of 2D inelastic plane stress elements).

References

[1] Kelly, J. M., Skinner, R. I., and Heine, A. J "Mechanisms of energy absorption in special devices for use in earthquake resistant structures, Bulletin of the NZ". *National Society for Earthquake Engineering*, Vol. 5(3), pp. 63-88, 1972.

[2] Skinner, R., Tyler, R. and Heine, A, "Steel beam dampers for increasing the earthquake resistance of structures". *7th World Conference, Istanbul*.

[3] Ciampi, V., Paolacci, F. and Perno, S, "Dynamic tests of a dissipative bracing system for seismic control of framed structures", *WIT Transactions on The Built Environment*, Vol. 23, 1996.

[4] Skinner, R. I., Robinson, W. H. and McVerry, G. H, *An introduction to seismic isolation*, John Wiley & Sons, 1993.

[5] Mezzi, M. and Parducci, A, "Seismic isolated bridges structures in Italy". *Earthquake Engineer 10th World*, Vol. 4, pp. 2199, 1992.

[6] Martinez-Rueda, J. E, "Cyclic response of a low invasivity bracing system for the passive control of framed structures", *13th World Conference on Earthquake Engineering*, Vancouver, B.C., Canada, Paper No. 951, August 1-6, 2004.

[7] Computer and Structure Inc, SAP2000, "Integrated finite element analysis and design of structures". *Computers and Structures, Inc*., Berkeley, California, USA, 2015.

[8] Park, R. and Sampson, R. A, "Ductility of reinforced concrete column sections in seismic design". *ASCE Journal of the Structural Division*, Vol. 69(9), pp.543-555, 1972.

[9] Oday Al-Mamoori, "Seismic redesign of precast portal frames using yield C-devices", *PhD thesis,* University of Brighton, School of Environment and Technology, 2018 (on going).

[10] Cofie, N. G. and Krawinkler, H, "Uniaxial cyclic stress-strain behavior of structural steel". *Journal of Engineering Mechanics*, Vol. 111(9), pp. 1105-1120, 1985.

[11] Martinez-Rueda, J. E., "Energy dissipation devices for seismic upgrading of RC structures". *PhD Dissertation*. Imperial College of Science, Technology and Medicine, Civil Engineering, 1997.

[12] ADINA, I, "Adina: A Finite Element Program for Automatic Dynamic Incremental Nonlinear Analysis". *ADINA Engineering Inc*, Watertown, MA, USA, 2016.

[13] Sussman, T. and Bathe, K.-J, "Studies of finite element procedures—stress band plots and the evaluation of finite element meshes". *Engineering computations*, Vol. 3(3), pp. 178-191, 1986.

[14] Ghabraie, K., Chan, R., Huang, X., Xie, Y., "Shape optimization of metallic yielding devices for passive mitigation of seismic energy". *Engineering Structures*, Vol. 32(8), pp. 2258-2267, 2010.

[15] Moradi, S. and Alam, M. S, "Finite-element simulation of post-tensioned steel connections with bolted angles under cyclic loading". *ASCE Journal of Structural Engineering*, Vol. 142(1), 2015.

[16] Jiao, Y., Saito, M. and Kohno, M, "Fatigue behavior of steel slit-dampers with various shapes". *16th World Conference on Earthquake Engineering, 16WCEE 2017*. Santiago Chile. N° 3542, 2017.